AGU ADVANCING EARTH AND SPACE SCIENCE

Water Resources Research

RESEARCH ARTICLE
10.1029/2021WR031755

Estimation of the Thermally Reactive Layer in Lakes Based on Surface Water Temperature

Marco Toffolon[1], **Azadeh Yousefi**[1], **and Sebastiano Piccolroaz**[1]

[1]Department of Civil, Environmental and Mechanical Engineering, University of Trento, Trento, Italy

Key Points:

- Only a portion of the lake volume reacts to the net heat flux exchanged at the surface, and this depends on stratification
- The size of the thermally reactive volume determines the thermal inertia and hence controls the warming rate at the surface
- The reactive volume depth is inversely dependent on surface water temperature through an exponential decay for direct stratification

Supporting Information:

Supporting Information may be found in the online version of this article.

Correspondence to:

M. Toffolon,
marco.toffolon@unitn.it

Citation:

Toffolon, M., Yousefi, A., & Piccolroaz, S. (2022). Estimation of the thermally reactive layer in lakes based on surface water temperature. *Water Resources Research*, *58*, e2021WR031755. https://doi.org/10.1029/2021WR031755

Received 7 DEC 2021
Accepted 27 MAY 2022

Author Contributions:

Conceptualization: Marco Toffolon, Sebastiano Piccolroaz
Data curation: Marco Toffolon, Azadeh Yousefi
Methodology: Marco Toffolon, Sebastiano Piccolroaz
Software: Marco Toffolon, Azadeh Yousefi, Sebastiano Piccolroaz
Supervision: Marco Toffolon
Validation: Marco Toffolon, Sebastiano Piccolroaz
Visualization: Marco Toffolon, Sebastiano Piccolroaz
Writing – original draft: Marco Toffolon, Azadeh Yousefi

Abstract How fast does lake surface water temperature (LSWT) react to climate warming or cooling? The thermal response of lakes varies with the season and, typically, day-to-day fluctuations are larger in summer. The reason is that lakes are stratified systems where the thermally reactive volume is smaller in summer and, hence, its heat capacity (thermal inertia) is reduced. We define the dimensionless parameter δ as the ratio between the surface volume reacting to the net heat flux through the air-water interface and the volume of the whole lake. By referring to a fully controlled case study obtained by means of a one-dimensional physically based model (Simstrat), we investigate the variability of δ throughout the year and its dependence on LSWT. Then, we compare the results with the parameterization adopted in the hybrid data-driven model *air2water*. Our analysis confirms that δ follows an exponential decay with increasing LSWT (i.e., a thinner surface layer in summer), and shows that this functional dependence varies between the warming and the cooling periods. These findings contribute to the understanding of the effect of a warming climate on water bodies and ecosystems by providing a simple tool to estimate the rate of change in lakes' water temperature.

Plain Language Summary The temperature of lake surface waters varies mostly because heat is exchanged with the atmosphere, in either direction. When heat is entering into the lake (spring-summer), it generates a surface layer with nearly uniform water temperature, which is almost isolated from the bottom by a region with localized temperature change. The rate of change of surface water temperature grows when the depth of this layer decreases, and is higher in summer when the vertical variation of water temperature is stronger. This produces positive feedback (water temperature tends to grow faster as it becomes warmer) that may exacerbate the effect of climate warming on lake ecosystems. In this analysis, we discuss how these dynamics can be parameterized as a function of lake surface water temperature, and we claim that this is a fundamental element that all simplified (bulk, statistical, etc.) lake models should include. The high performance of a model based on this concept, and that has been extensively applied (*air2water*), supports this argument.

1. Introduction

The dynamics of water temperature in lakes have been extensively investigated in the last decades because of their ecological relevance and the possibility to study temperature trends as a local effect of climate change acting at the global scale (e.g., Hondzo & Stefan, 1993; Sahoo et al., 2016). The surface water's equilibrium temperature, that is, the temperature at which the net heat flux exchanged at the lake's surface is zero, reacts approximately as 70%–85% of the rate of change of air temperature according to Schmid et al. (2014), which means a potential increase by about 1.0–1.2 to 3.1–3.7 in 2081–2100 relative to 1850–1900, according to a best estimate increase of global air temperature of 1.4 and 4.4°C under the most optimistic SSP1-1.9 scenario and the most severe SSP5-8.5 scenario, respectively (IPCC, 2021). Consequences can be severe: change of lake's regime from dimictic to monomictic (e.g., Ficker et al., 2017), alteration of stratification timing (Woolway et al., 2021) and strength, with consequences on deep water temperature (Anderson et al., 2021), increase of the chance of summer hypoxic conditions and cyanobacterial blooms (e.g., Paerl & Huisman, 2008), deterioration of the quality of drinking water (e.g., Delpla et al., 2009), problems with fisheries (e.g., Butcher et al., 2015), and alteration of ice-covered periods (e.g., Magnuson et al., 2000). In this context, the climatic effects can also interact with anthropogenic pressures, making the impacts on lakes' ecosystems even more threatening.

The physical process governing water temperature can be described in a relatively simple way by considering a bulk model for the whole lake. Different heat fluxes are exchanged through the lake boundaries with the atmosphere (Lofgren & Zhu, 2000), sediments (Fang & Stefan, 1996), inflows, and outflows. The resulting net

Writing – review & editing: Marco Toffolon, Azadeh Yousefi, Sebastiano Piccolroaz

heat flux produces a change in the average temperature that is inversely proportional to the lake's heat capacity (Toffolon et al., 2014). Hence, the larger the water volume is, the smaller the temperature change that is produced by a given net heat flux.

The consequence of such a simple physical argument is that density stratification heavily affects the thermal response of lake surface water temperature (LSWT) (Calamita et al., 2021; Piccolroaz et al., 2015; Woolway & Merchant, 2017; Zhong et al., 2016). In stratified conditions, the surface layer is almost thermally isolated from the water underneath, and LSWT changes are dominated by the heat fluxes exchanged with the atmosphere. Density depends mostly on water temperature in freshwater lakes, so that positive feedback exists between LSWT increase during the warm season and the strengthening of the stratification (Piccolroaz et al., 2015). The development of a well-mixed surface layer, which becomes increasingly more isolated from the lower layers moving from spring to summer, has the effect of reducing the volume of water affected by the heat exchange, thus enhancing the warming rate of LSWT. Such positive feedback creates a steepening of LSWT warming after the transition through uniform density conditions (in dimictic lakes, when LSWT approaches the temperature of maximum density $T_{md} = 4$°C). An example of such feedback is discussed for the case of Lake Superior by Piccolroaz et al. (2015) and Zhong et al. (2016) through independent model-based sensitivity analyses. This is also the mechanism at the basis of the amplified response of LSWT to air temperature variation that has been observed in deep lakes (Woolway & Merchant, 2017) and, more precisely, in the pelagic zones of deep lakes (Calamita et al., 2021) in the presence of the anticipation of the stratification season.

The physical process of formation and disruption of stratification is likely the most critical feature that a lake thermal model should include and be able to properly simulate to predict how LSWT reacts to the net heat flux. A typical hysteresis between LSWT and air temperature can be noticed especially in deep lakes (Toffolon et al., 2014). In this respect, purely statistical models struggle to represent such dynamics in a correct way, unless through accounting for different regression functions in the different seasons (e.g., McCombie, 1959). Hence, hybrid models have been developed that blend together a physically constrained description of the processes together with a data-driven approach to evaluate the model parameters. An example is the *air2water* model (Piccolroaz et al., 2013). In that model, the stratification intensity is expressed by means of a dimensionless ratio, δ, of the volume of the thermally reactive layer relative to that of the whole lake. The functional dependence of δ on LSWT assumed in *air2water* is simple (an exponential decay) but has been proved to provide good results in terms of the overall dynamics, and to compare well with independent definitions of the epilimnion of the lake based on observed water temperature profiles (Piccolroaz et al., 2015; Toffolon et al., 2014).

The aims of this work are: (a) providing a reasonable definition of the thermally reactive volume based on the variability of LSWT; (b) understanding how its depth compares with other definitions of the surface layer (e.g., epilimnion thickness); (c) testing whether the performance of a model like *air2water* can be improved by modifying the simplified functional dependence of δ on LSWT assumed so far; (d) investigating the role of lake's morphological features, and in particular the depth, on the response of δ to LSWT. To have full control on the variables involved, the analysis is based on the results of a numerical model, Simstrat (Goudsmit et al., 2002), and not directly on observations. The simulated temperature profiles are used to compute δ in this synthetic case study and to verify the functional dependence assumed in *air2water*. Finally, the dynamics of the thermally reactive layer are discussed with reference to observations from a real lake.

2. Materials and Methods

2.1. Heat Budget of the Surface Layer

The heat budget of a lake can be set as an equation that balances the change of internal energy and the total flux of energy through the boundaries:

$$\frac{d}{dt}\left(\rho\, c_p V_{tot} T_{av}\right) = P_{net} \tag{1}$$

where V_{tot} [m^3] is the total volume, T_{av} [°C] is the lake-averaged, volume-weighted water temperature, P_{net} [J day^{-1}] is the net total heat flux that is exchanged through the entire boundary surface of the lake, ρ [kg m^{-3}] is water density, c_p [J kg^{-1} K^{-1}] is the heat capacity of water at constant pressure, and t [day] is time. Neglecting (as a first approximation) the change of volume and thermodynamic properties of water with time, the rate of change

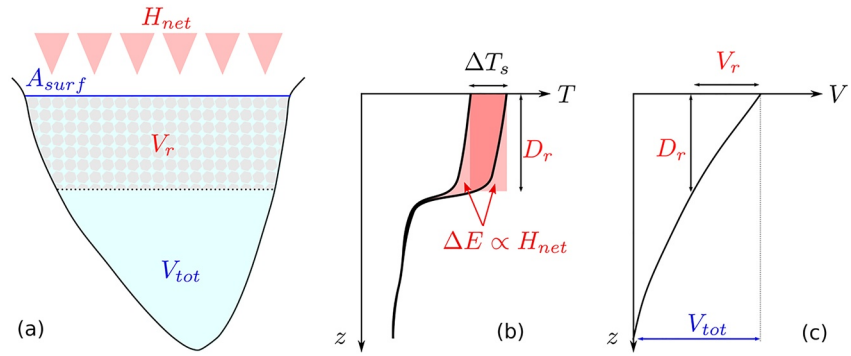

Figure 1. (a) Conceptual sketch of the thermally reactive layer with volume V_r and depth D_r being connected by the hypsometric curve $V(z)$. The two temperature profiles in (b) show the T change in a given period Δt (1 day in our model) caused by a net energy gain $\Delta E = A_{surf} H_{net} \Delta t = \rho\, c_p\, V_r\, \Delta T_s$, where the second equality is the discretization of Equation 3. Note that a positive net heat flux, H_{net}, determines an energy gain in the lake, ΔE, which is reflected in a proportional temperature change (shaded areas: between the two profiles and the equivalent rectangle with edges ΔT_s and D_r). The depth D_r depends on V_r via the hypsometric curve (c), $V(z)$. The case of net energy loss is analogous.

of the average water temperature can be estimated by isolating dT_{av}/dt in Equation 1. Introducing the additional simplification that $P_{net} \cong A_{surf}\, H_{net}$, that is, limiting the total energy flux to the net exchange through the free surface, where H_{net} [J m^{-2} day^{-1}] is the net heat flux per unit area (assumed positive if the flux enters into the lake, i.e., warming) and A_{surf} [m^2] is the surface area, we obtain

$$\frac{dT_{av}}{dt} = \frac{A_{surf}}{\rho\, c_\rho\, V_{tot}} H_{net} \tag{2}$$

Equation 2 describes the behavior of a variable, T_{av}, that does not have a direct physical correspondence, unless the water body is homothermal. However, homothermal conditions are not the normal state of a lake.

Indeed, lakes are typically characterized by the presence of relatively well-mixed layers separated by regions where the density gradients are large due to the vertical variability of water temperature. Hence, for practical applications, more relevant than T_{av} is the temperature of the surface layer, where light penetrates and several important ecological processes occur. For these reasons, here we focus on the surface layer and we refer to LSWT to indicate the temperature of the water in this layer.

Defining the surface layer and the associated LSWT is not trivial. It is sufficient to mention that, in the field, LSWT is traditionally measured with conventional thermistors from ships, buoys, or moored stations at depths from centimeters to a couple of meters below the lake surface (bulk temperature). Satellite infrared radiometers are also used to get a measure of the temperature of the very thin surface layer, which in this case is approximately on the order of 10 μm (skin temperature; Nehorai et al., 2013). Bulk and skin temperatures are correlated, although the differences between the two can be on the order of a few degrees depending on the time of the day and on the meteorological conditions (Prats et al., 2018; Wilson et al., 2013).

In the present analysis, we refer to the bulk measure of LSWT, as it is more representative of the average temperature in the surface layer when it is well-mixed. Then, we set up a simplified heat budget for this surface layer in the form of

$$\frac{dT_s}{dt} = \frac{A_{surf}}{\rho\, c_p\, V_r} H_{net} \tag{3}$$

where T_s [°C] is LSWT. We note that Equation 3 is an operational definition of the volume V_r [m^3] of the "thermally reactive" surface layer (Figure 1). We also acknowledge that this definition is inherently dependent on where/how LSWT is measured, and we speculate that it approximately corresponds to the surface well-mixed layer (i.e., the epilimnion), an equivalence that will be tested in the following analysis.

The choice of the time step used to discretize the heat budget Equation 3 is important. A natural choice is to use a daily (diel) time step, as it allows for neglecting the temporary stratification that can develop in the warmer

hours (especially in summer). It is necessary to note that the simplified heat budget (Equation 3) neglects the heat exchanged with the deeper volume of the lake and the contribution of inflows and outflows. These terms can be estimated and added on the right-hand side of Equation 3 but are neglected in this analysis. Moreover, as for Equation 2, the surface heat budget (Equation 3) assumes that the temporal variation of the volume V_r is of minor importance so that this term can be extracted from the time derivative.

2.2. Estimate of the Thermally Reactive Layer

Equation 3 is the conceptual basis of the *air2water* model, which adopts a largely simplified version of this heat budget amenable of inclusion in a data-driven hybrid model. It is not necessary to discuss the explicit formulation of the *air2water* model, for which the reader can refer to the original papers (Piccolroaz, 2016; Piccolroaz et al., 2013; Toffolon et al., 2014) and the subsequent ones where the model has been successfully adopted in several lakes worldwide (Calamita et al., 2021; Czernecki & Ptak, 2018; Flaim et al., 2020; Javaheri et al., 2016; Piccolroaz et al., 2015, 2018, 2020, 2021; Prats & Danis, 2019; Schmid & Köster, 2016; Wood et al., 2016; Zhu et al., 2020, 2021) also as an impact model in the ISIMIP Lake Sector (Golub et al., 2022). It suffices to say that the volume of the thermally reactive layer in Equation 3 changes in time depending on stratification, and the variation is described by the dimensionless parameter

$$\delta = \frac{V_r}{V_{tot}} \tag{4}$$

The key element of the *air2water* model is the assumption that δ dominantly depends on LSWT. In particular, the stratification parameter is expressed by means of a simplified exponential relation,

$$\delta\,(T_s) = \exp\left(-\frac{T_s - T_h}{a}\right), \tag{5}$$

where T_h is the deep hypolimnetic temperature ($\cong T_{md}$ for dimictic lakes) and a is a calibration parameter that physically represents the temperature range over which δ decreases with the temperature T_s. A small value of a implies that a modest increase of T_s is sufficient to reduce δ to small values; a large value of a suggests that δ tends to be insensitive to LSWT as generally occurs in particularly shallow lakes where almost the entire lake volume participates to the heat exchanges throughout the year (i.e., $V_r \approx V_{tot}$ and $\delta \approx 1$). In this analysis, we refer to the 6-parameter version of the model and assume $\delta = 1$ for $T_s < T_h$. Thus, we do not study the evolution of the thermally reactive layer for inverse stratification (for more details, see Piccolroaz et al. (2013)). The value of the parameter a (denoted as a_4 in Toffolon et al. (2014), and following contributions) is selected, together with the other model's parameters, by calibrating the *air2water* differential equation using optimization algorithms (not shown) and relying on the available LSWT data. The following analysis aims at testing the appropriateness of relationship (Equation 5) and its possible improvement.

From a practical point of view, the value of δ can be computed by combining Equations 3 and 4:

$$\delta = \frac{H_{net}}{\rho\, c_p\, D_{av}} \left(\frac{dT_s}{dt}\right)^{-1} \tag{6}$$

where $D_{av} = V_{tot}/A_{surf}$ is the mean depth of the lake, and the surface temperature variation dT_s/dt can be estimated using observations or numerical results.

The role of thermal inertia on the thermal response can be highlighted by recasting Equation 6 in dimensionless terms:

$$\sigma\, \delta \frac{dT_s^*}{dt^*} = H_{net}^* \tag{7}$$

where $T_s = T_0\, T_s^*$ with T_0 the range of temperature variability, $H_{net} = H_0\, H_{net}^*$ with H_0 a reference value of the daily averaged net heat flux through the year, $t = t_y\, t^*$ with $t_y = 365 \times 86{,}400$ s the duration of a year, that is, the typical time scale of the investigated problem. The dimensionless parameter

$$\sigma = \frac{\rho\, c_p\, D_{av}\, T_0}{H_0\, t_y} \tag{8}$$

depends on D_{av} and does not change significantly in time for most of the cases (coherent with assuming constant thermodynamic properties of water), whereas δ and H^*_{net} are functions of T^*_s and (the latter) of the meteo-climatic conditions, and hence of time. Just as a reference, assuming standard values of ρ and c_p for water and $H_0 \cong 200$ W m^{-2}, we obtain $\sigma \cong D_{av}$/(300 m).

If $\sigma \ll 1$, as in shallow lakes, the temporal derivative may be neglected and models based on the concept of equilibrium temperature (Schmid et al., 2014), that is, the time-varying LSWT that satisfies the condition $H_{net} = 0$, can be adopted. If σ is not sufficiently small ($\sigma \sim 10^{-1}$ is a typical order of magnitude, as for many lakes $D_{av} \sim$ 30 m), the thermal inertia can play a significant role making the concept of equilibrium temperature no longer valid. The relevance of the thermal inertia is seasonally expressed by the parameter δ, which becomes small when a strong stratification develops. Typical values of the epilimnion depth in summer are ~10 m, so δ can drop below $\sim 10^{-1}$ for a relatively deep lake, while $\delta \sim 1$ when it undergoes seasonal convective mixing. Thus, we expect that equilibrium temperature models can be acceptable approximations in very shallow lakes year-round, and in relatively deep lakes only in summer but not in the other seasons.

2.3. Estimate of the Surface Layer From Temperature Profiles

The typical way to estimate the depth of surface volume is by looking at the vertical distribution of water density, which is mostly dependent on water temperature, $T(z)$, where z is the vertical coordinate. Different definitions of this depth are possible (Wilson et al., 2020), but all are intrinsically related to the definition of a strong temperature gradient (i.e., the thermocline) that produces a strong density gradient (pycnocline). The thermocline separates an approximately uniform layer above, the epilimnion, from a relatively calm layer below, the hypolimnion. The thermocline depth can be identified by the position of the largest value of the temperature gradient, $max\{|dT/dz|\}$, where the absolute value is included to also consider the case of inverse stratification in winter ($T < T_{md}$). We arbitrarily assume 0.1°C/m as a lower threshold for the existence of the thermocline.

After identifying the position of the thermocline, the lower limit of the epilimnion is estimated as the intersection between the line with the slope of the maximum gradient passing by the thermocline and the vertical line corresponding to LSWT (see Section S2 and Figures S1 and S2 in Supporting Information S1). Any depth can be converted into a volumetric ratio by means of the hypsometric curve, $V(z)$. Accordingly, we define the volumetric ratio δ_{thcl} for the thermocline depth, and δ_{epil} for the bottom of the epilimnion.

From a physical point of view, the volumetric ratios (δ_{thcl} and δ_{epil}) obtained from the analysis of a temperature profile and the volumetric ratio (δ) based on the heat budget and computed by means of Equation 6 are conceptually different. Hence, we use subscripts to define the different volumetric ratios. Given the morphological characteristics of the lake and the net heat flux H_{net}, Equation 6 provides a coherent procedure to compute δ once the temporal variability of LSWT is known. As anticipated earlier, this estimate of δ is intrinsically dependent on where/how LSWT is defined; nevertheless, as a first approximation, we assume that LSWT is nearly homogeneous within the well-mixed epilimnion. This evaluation of δ can be applied to a real case, although large uncertainties may exist especially in the quantification of the net heat flux. In the following analysis, we exploit the results of a physically based one-dimensional model in order to have full control of all variables involved in the definition (6). Moreover, the use of a synthetic case study allows for testing different geometrical and climatic configurations, and, accordingly, for exploring how different factors affect the estimate of δ.

2.4. Reconstruction of the Thermal Dynamics

The model used for the reconstruction of the thermal dynamics in the synthetic case study is Simstrat (Goudsmit et al., 2002), a well-established one-dimensional mechanistic model. Simstrat has been successfully applied in several lakes and is used as a real-time tool to analyze the behavior of several Swiss lakes (Gaudard et al., 2019, see also https://simstrat.eawag.ch/). Here, we used it to simulate the thermal dynamics in an artificial case study that has the same dimensions as Lake Zurich and the corresponding meteorological forcing; in this way, we were able to explore all the features of δ estimated from Equation 6. To simplify the analysis, however, we removed rainfall, inflows, outflows, and the geothermal heat flux, thus restricting the evaluation to the net heat flux exchanged through the lake surface. The heat flux's terms were computed according to the relations implemented in Simstrat with the measured meteorological variables. Therefore, the simulated variables may not exactly match

actual values, but this is not the objective here. The main features of the case study are reported in Table S1 in Supporting Information S1; see also Figures S4, S10, and S21 in Supporting Information S1.

Additionally, we considered two variations of the reference lake based on a vertical shrinking that keeps all the other factors (meteorological forcing, surface area, etc.) unaltered. While in the original (deep) Lake Zurich, the maximum depth is 136 m, we artificially built a shallow (depth 10 m) and an intermediate (50 m) lake by stretching only the vertical coordinate. This allows us to explore the effect of the depth on the stratification simulated with Simstrat.

The Simstrat model was run with a time step of 300 s and the results were saved every 2 hr; the vertical grid was equally spaced with intervals of 1 m (in all cases). For the analysis at the daily scale, water temperature profiles were extracted every 24 hr (at midnight) and daily integrated values of the net heat flux H_{net} were computed based on the 2-hr output of short-wave (penetrating) incoming radiation, long-wave incoming, and emitted radiation, and fluxes of latent and sensible heat. Reflected radiation (albedo) was subtracted from the radiative fluxes as in Simstrat. Only the fraction absorbed by the water column (depending on water transparency) was considered for the short-wave component, because the current version of Simstrat does not include a sediment layer that could store the heat penetrating down to the bottom (relevant only for shallow and transparent lakes). The LSWT was taken as the temperature of the upper layer of model (thickness 1 m).

The values of LSWT and H_{net} were used to compute δ according to Equation 6, and the range was limited to 0–1. In fact, the values of δ obtained directly from the simulation, which will be indicated hereafter simply as "data," were characterized by large fluctuations from day-to-day. To remove them, a "smooth" version of LSWT and δ (all definitions) was obtained as the median value in a moving window of 15 days. Parallel to the computation of δ, the analysis of the temperature profiles provided the estimates of δ_{thcl} and δ_{epil} based on the position of thermocline and epilimnion bottom. Moreover, the "climatological year" (denoted as "c.y." in the following figures) was computed for all variables as the average of the values in each day of the year (DOY) over the whole time series (e.g., Toffolon et al., 2020). When the number of valid values in a DOY was lower than 5, the corresponding term in the climatological year was not computed, a condition that in our case occurred only when the thermocline was not present.

Finally, the *air2water* model, in its 6-parameter version (Toffolon et al., 2014), was applied to the time series of LSWT simulated by Simstrat. The model's parameters were calibrated by minimizing the root mean square error (RMSE) between simulated and reference LSWT to obtain the value of the parameter a used in Equation 5.

Alternative versions of Equation 5 were also tested (see Section S3 in Supporting Information S1 for the options and the following section for the results). We anticipate that the best results were obtained by modifying the original formulation introducing an asymptotic value a_{as} for the cooling phase ($dT_s/dt < 0$), and defining a similar exponential law for the warming phase ($dT_s/dt > 0$):

$$\delta = \begin{cases} a_{as} + (1 - a_{as}) \exp\left(-\dfrac{T_s - T_h}{a}\right) & \text{for} \quad \dfrac{dT_s}{dt} < 0 \\ a_{as} + a_{\delta} \exp\left(-\dfrac{T_s - T_h}{a_T}\right) & \text{for} \quad \dfrac{dT_s}{dt} > 0 \end{cases} \tag{9}$$

where a_T and a_δ are additional parameters to be calibrated; note that $\delta = 1$ for $T_s < T_h$ in the cooling phase, but it can be larger or smaller for the warming phase. No multiplying coefficient was introduced in Equation 5 to avoid overparameterization in the model (see the discussion in Piccolroaz et al. (2013) and Piccolroaz (2016)); similarly, only one of Equation 9 includes parameters that can make the maximum δ different from 1. The cooling and warming phases are defined by computing dT_s/dt within an interval of 5 days before the current time. With the introduction of three new parameters, this modified version of *air2water* contains 9 degrees of freedom.

3. Results

3.1. Thermal Dynamics of the Surface Layer

The analysis of the 33-year-long series of daily LSWT values allowed for a plausible characterization of the thermal dynamics in the "artificial" Lake Zurich; in this first part of the results, we refer to this original (deep) case. Figure 2 illustrates the variability of LSWT and δ for 3 years, characterized by significant inter-annual variability.

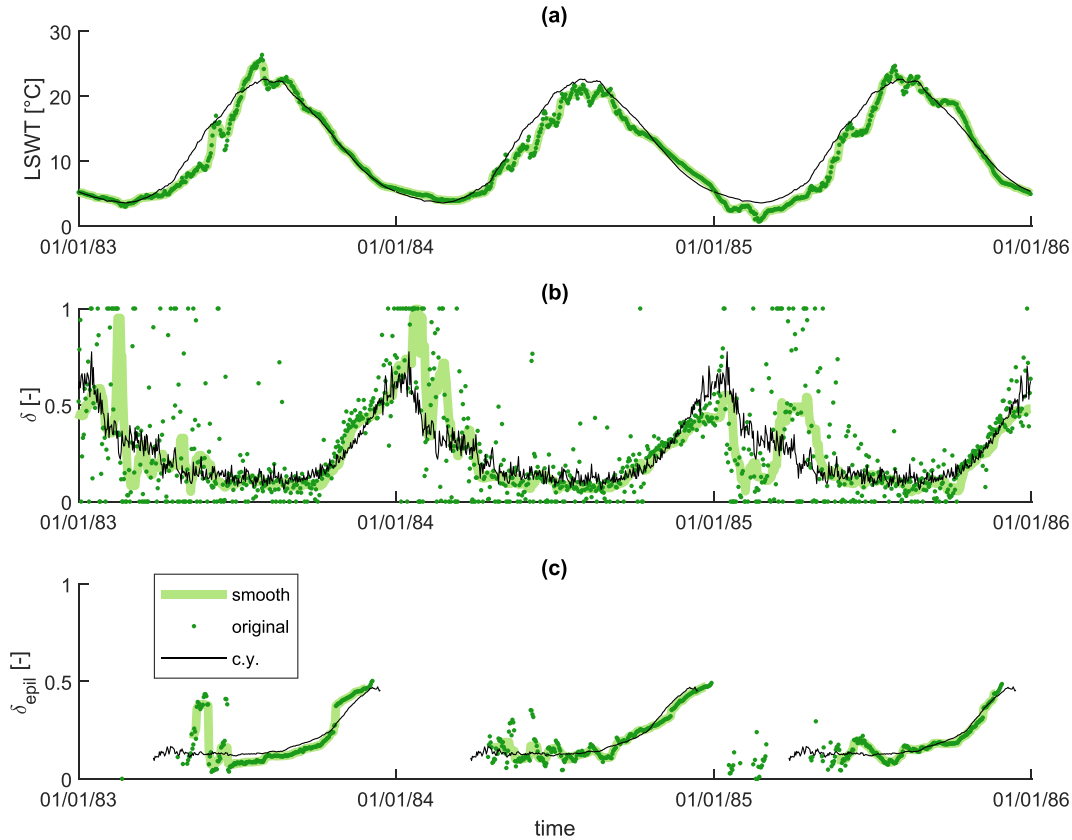

Figure 2. Evolution of simulated LSWT and δ in 3 years (1983–1985): (a) LSWT, (b) δ computed from the heat budget, (c) δ_{epil} computed from the temperature profile as the bottom of the epilimnion. The values obtained at the daily time step (referred to as "original" in the legend) are plotted together with the 15-day moving average (smooth) and the climatological year ("c.y.," defined only when at least 5 values were available for each DOY), which is repeated for the 3 years. The data of the deep case (maximum depth 136 m) are shown in this figure and in the following ones, where not otherwise explicitly stated. Similar plots for the other cases (intermediate and shallow) are reported in Figures S11 and S22 in Supporting Information S1. LSWT, lake surface water temperature.

All plots include the original data, the smoothed time series, and the climatological year repeated identically three times. It appears that the climatological year describes the LSWT behavior at the first order of approximation, but the actual values may differ significantly throughout the seasons (Figure 2a). The differences between actual and climatological values clearly emerge also when looking at the values of δ computed from the heat budget (Figure 2b). Anyway, the general trend shows that δ is smaller during the stratified period in summer, when it can be one order of magnitude smaller than during the mixing periods in winter. This means that the thermally reactive volume is limited in summer (small δ) and grows in winter (δ approaching 1). The value of δ_{epil} obtained from the temperature profiles (Figure 2c) shows a smaller intra-annual variability, with an increase up to values around 0.5 only during the destratification period in autumn. The absence of values in the winter period is due to the absence of a well-defined thermocline (the temperature gradient being below the considered threshold).

The difference between the values of δ based on the heat budget (6) and δ_{epil} estimated from the temperature profiles may raise the question of whether the two definitions are consistent with each other. Figure 3 shows the relationship between them in a scatter plot parity diagram, where the points corresponding to the mean year have been subdivided into periods of increasing LSWT (rising limb of the curve in Figure 2a, i.e., warming) and decreasing LSWT (falling limb, i.e., cooling). Most of the data in the cooling phase (see the blue dots referring to the climatological year in the plot) lie below the parity line. In fact, the volume ratio δ_{epil} obtained from the temperature profiles tends to be slightly larger (i.e., deeper) than δ obtained from the heat budget. The behavior is different in the warming phase (red dots): δ_{epil} is approximately constant (while its variability is large in the cooling phase), but δ from the heat budget varies significantly and can be larger than δ_{epil}.

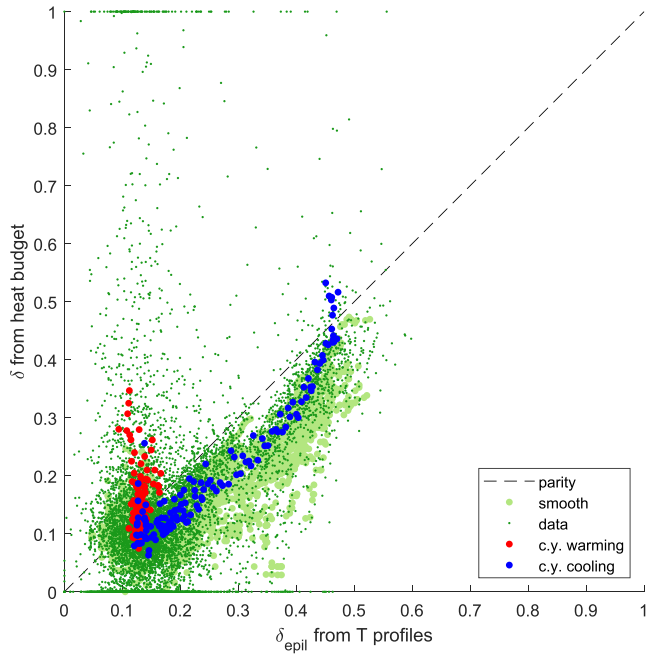

Figure 3. Comparison between the values of δ_{epil} obtained from the simulated temperature profiles (epilimnion depth) and those from the heat budget, δ. The original daily values are plotted together with those of the smoothed time series and of the climatological year, separated into the warming and cooling periods.

The analysis of Figure 3 suggests that the thermally reactive layer (associated with δ) tends to be smaller than the usual definition of the epilimnion (δ_{epil}) during the cooling period. Indeed, in this period, there is a progressive deepening of the thermocline caused by convection driven by surface cooling. One may expect that the two definitions tend to coincide because the epilimnion is typically well-mixed in this period; however, the surface volume that loses heat is slightly smaller. Hence, the temperature decrease can be slightly higher than what is expected based purely on the epilimnion depth. The difference, however, is modest and the correlation between δ and δ_{epil} is evident.

Conversely, when stratification is forming (warming phase), the heat flux affects a volume that is larger than the volume of the epilimnion, which is approximately constant. Such a difference can be explained by the reduced strength of the thermocline in this phase and the possibility to have multiple thermoclines along the water column. Here, we consider only the thermocline with the highest gradient (different definitions are possible, and would lead to partially different considerations), which is often the shallowest because the progressive heating of the surface is the leading mechanism. Nevertheless, the stratification is not stable and the insulating effect is limited, thus the thermally reactive layer may also extend well beyond the epilimnion.

Considering δ_{thcl} obtained from the position of the thermocline instead of the depth of the epilimnion does not modify the overall picture. As expected, it can be shown (see Figures S5, S14, and S25 in Supporting Information S1) that δ_{thcl} based on the thermocline is always larger than δ_{epil} corresponding to the epilimnion, but the two definitions are correlated.

The visual inspection of Figure 2 suggests that LSWT changes are stronger when δ is small due to reduced thermal inertia, as already suggested by Toffolon et al. (2014) and Piccolroaz et al. (2015). It is therefore interesting to analyze the relationship between the temporal variability of LSWT and that of the lake-averaged temperature predicted by Equation 2. As we consider the results of the numerical simulation with Simstrat, the analysis benefits from the knowledge of all variables, so it is straightforward to compute T_{av}. Figure 4 shows how the simulated time derivative of water temperature (vertical axis) compares with the right-hand side of Equation 2 (horizontal axis), which corresponds to the prediction of dT_{av}/dt based on the net heat flux H_{net} for the total lake volume.

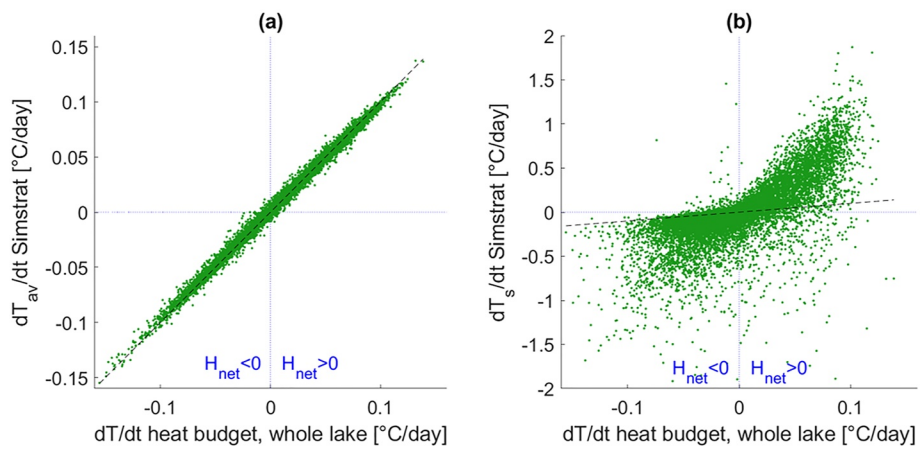

Figure 4. Comparison between the rate of change of water temperature simulated by Simstrat for (a) lake-averaged temperature and (b) LSWT, against the theoretical change of temperature that is computed using H_{net} in the heat budget for the whole lake, described in Equation 2. The dashed 1:1 parity line indicates the perfect agreement between the two definitions. LSWT, lake surface water temperature.

As expected, dT_{av}/dt simulated by Simstrat is almost identical to the temperature change estimated from H_{net} for the whole lake based on Equation 2 (Figure 4a). Conversely, when we consider the simulated change of LSWT (which we recall is the water temperature of the upper 1 m layer), dT_s/dt, against the temperature change estimated from H_{net}, we notice a much more disperse cloud of points (Figure 4b), which deviates from the parity line. In fact, the slope of the upper envelope of the cloud is approximately one only on the left-hand side of the plot (negative H_{net}, i.e., cooling, mostly associated to destratification), while it is about 10 in the right-hand side (positive H_{net}, i.e., warming, mostly associated to summer stratification). Although a large spread exists, the general trends suggest a significantly different behavior in the cooling and warming periods (based on the sign of H_{net} now). In fact, the thermally reactive volume is smaller in stratified conditions and makes LSWT grow or decrease more rapidly than what would be expected if the whole lake reacted uniformly. Figure 4b suggests that stratification is typically developed in the warming phase, where most of the points lay above the parity line. Conversely, a more variable behavior characterizes the cooling phase, with some points aligned on the steep slope and others on the parity line. The latter case is consistent with conditions when the reactive volume is large and approaching the volume of the whole lake, hence when T_s tends to coincide with T_{av}.

The analysis of Figure 4 suggests some interesting considerations. Equation 2 establishes a proper physical correlation between the net heat flux entering/leaving the lake ($H_{net} \gtrless 0$) and the average warming/cooling ($dT_{av}/dt \gtrless 0$), and this is clearly shown in Figure 4a. Differently, this direct correlation is not strictly satisfied for LSWT changes, as considered in Equation 3: in fact, Figure 4b shows several points in the region where Simstrat simulates a surface cooling ($dT_s/dt < 0$) even if heat enters into the lake ($H_{net} > 0$, i.e., in the lower right quadrant of the plot). The reason for this counterintuitive response lies in the temporal variability of the surface volume: for instance, a strong wind can mix and deepen the surface layer producing a decrease in LSWT even if the net heat flux is positive. Similarly, convection due to night cooling can also contribute to increase the depth of the thermally reactive layer even in the presence of daylight warming (we recall that LSWT is taken at midnight).

3.2. Estimate of δ as a Function of LSWT

The results presented in the previous section can be condensed into a single picture highlighting the intra-annual variability. Figure 5 shows the complete time series of LSWT and δ as a function of DOY, including the original data, the smoothed time series, and the climatological year subdivided into the warming and cooling periods. In the following analysis, we consider the definition of δ based on the heat budget, Equation 6. For the interested reader, the corresponding analysis for δ_{epil} defined as the epilimnion depth is reported in Figure S6 in Supporting Information S1.

A careful analysis of Figures 5a and 5b shows that the temporal variation of δ does not exactly match that of LSWT among the warming and cooling periods. To better illustrate the dependence between these two variables, in Figure 6 we plot the values of δ as a function of LSWT computed at the same DOY: a hysteretic behavior is evident, highlighting a variable relation between δ and LSWT (see Figure S7 in Supporting Information S1 for the analogous relationship between δ and LSWT). Therefore, the use of a bijective function between δ and LSWT, as in *air2water*, might seem questionable. The distinction between the periods of increasing and decreasing LSWT supports the identification of a different mechanism for the thermal response of the lake in the warming (spring-summer) and cooling (autumn-winter) seasons.

Starting from homothermal conditions (4°C), LSWT follows a fast rise because stratification tends to be closer to the surface in spring-summer (Figure 5c), and a shallow surface layer owns a lower thermal inertia (small δ) that accelerates the process. In late summer and autumn, the surface layer deepens as soon LSWT decreases due to partial convective overturns. Therefore, for the same value of LSWT, the value of δ is larger in the cooling than in the warming phase.

3.3. Testing Alternatives for δ in *air2water*

Having appreciated that the relationship between δ and LSWT is different between the warming and cooling periods, one may wonder how the *air2water* model can work effectively given that it includes a univocal LSWT-δ parameterization. Therefore, we calibrated the *air2water* model as described in Piccolroaz (2016) using daily values of LSWT from Simstrat as predictand and the same air temperature used in Simstrat as external forcing. The functional dependence of δ based on Equation 5 after calibration of the parameter a is depicted as a black

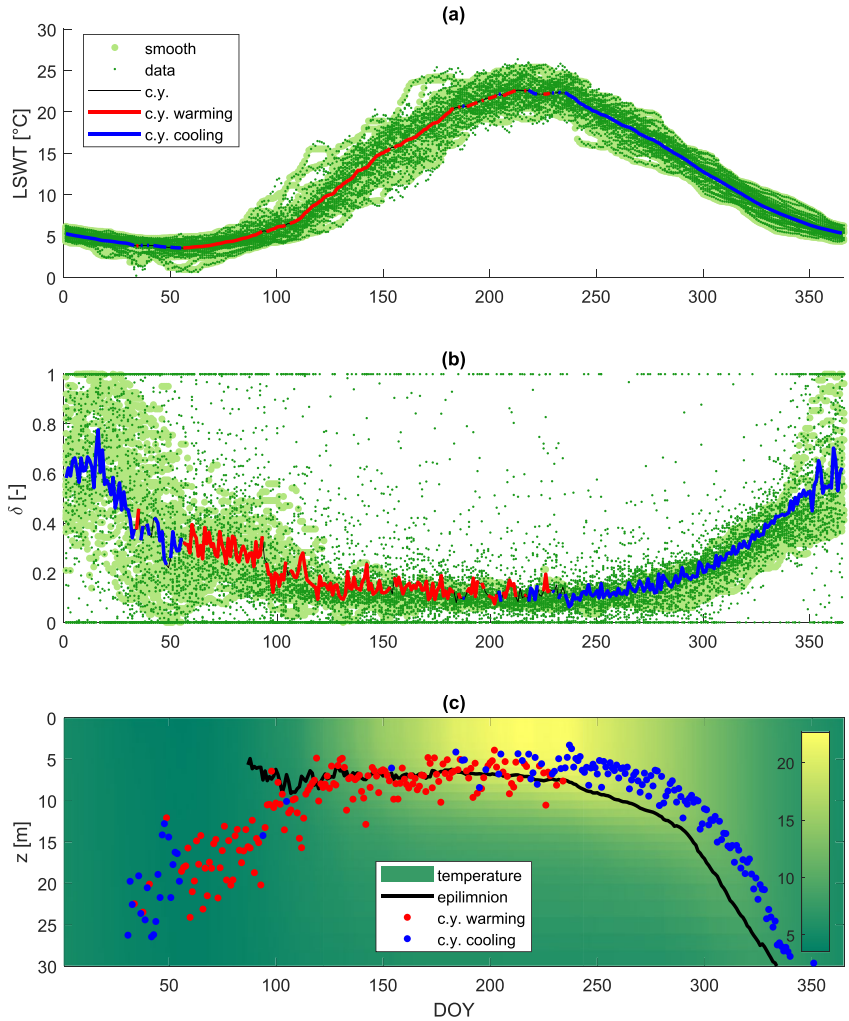

Figure 5. Seasonal variability of (a) simulated LSWT and (b) δ obtained from the heat budget Equation 6 as a function of the day of the year (DOY) for all years (all points are plotted). Both the original daily values and the smoothed data are indicated. The values for the climatological year are separated into warming (red) and cooling (blue) periods. (c) Simulated water temperature of the climatological year as a function of depth (limited to the first 30 m of the "deep" case study) and time. The black line represents the average position of the bottom of the epilimnion. Dots indicate the depths of the thermally reactive layer based on δ obtained from the heat budget Equation 6. LSWT, lake surface water temperature.

curve in Figure 6. The curve represents a sort of upper limit for the values of δ computed from the heat budget (Equation 6), suggesting that the optimization of the *air2water* parameters tends to maximize the estimated values of δ. This allows for reducing the excessive fluctuations that would result from smaller values of δ and that could penalize the performance of the model. Hence, the global optimization used in *air2water*, considering the impossibility to follow the LSWT exactly, brings to a smooth prediction of the LSWT time series.

As already mentioned, we tested different alternative formulations for the parameterization of δ as a function of LSWT in *air2water* to obtain better results. After calibration of the modified versions of *air2water*, we found that Equation 9 provides good results while being structurally similar to the original model. The dual-functional dependence (Equation 9) is shown in Figure 6 by the red (warming) and blue (cooling) curves. It appears that the curve for the cooling period covers the whole range of δ for LSWT above approximately 5°C is, while the curve for the warming period suddenly drops to the value of $\delta < 0.4$ as soon as stratification develops above 4°C. Interestingly, the climatological year (blue dots) shows a steep drop of δ at the end of the cooling period (left-hand side) between 3 and 4°C, when the inverse stratification starts developing. Describing the functional dependence of δ in this period is, however, beyond the scopes of this contribution, and we keep the simplified condition $\delta = 1$ characterizing the 6-parameter version of *air2water*.

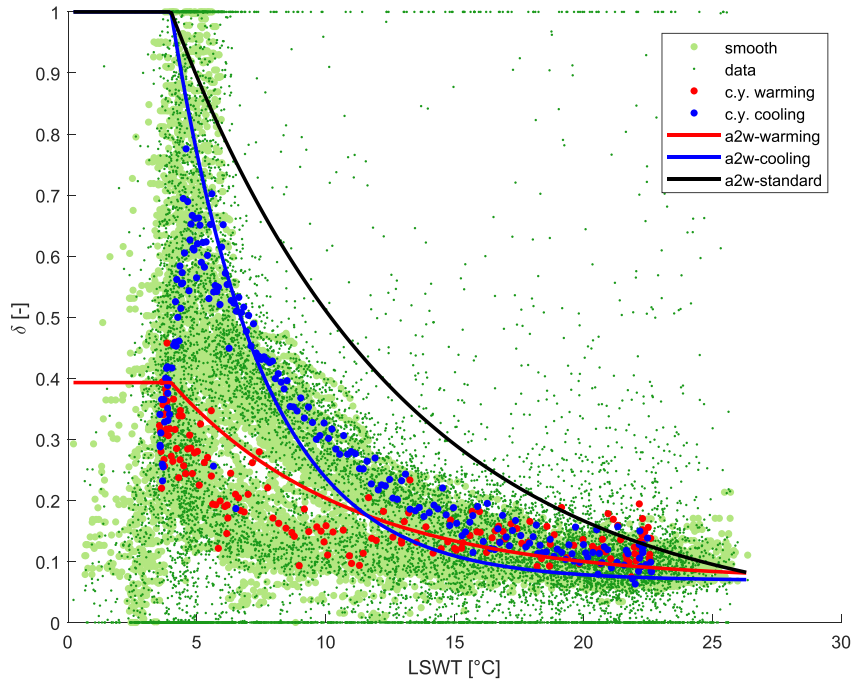

Figure 6. Estimates of δ computed from the heat budget (Equation 6) as a function of the simulated LSWT for the whole record (original daily values and smoothed time series) and for the climatological year (separated into warming and cooling period). The functional dependences of δ on LSWT modeled by Equations 5 and 9 are plotted as a reference to the empirical relations used in *air2water*. LSWT, lake surface water temperature.

Then, the question arises as to how significant is the use of two distinct functions for the dependence of δ on LSWT? As reported in Table 1, the new version performed better, with an RMSE = 0.892°C to be compared to an RMSE = 0.961°C of the standard version (i.e., an improvement of 7%). We note that the better performance is reached thanks to the improved description of the physical process, and not purely to the increased number of model's parameters. This is confirmed by the significantly better score of the Akaike Information Criterion (AIC) of the modified model (Sakamoto et al., 1986). Different formulations for δ (see Section S3 in Supporting Information S1) did not yield better improvements.

Finally, we show Figure 7 as an example of the different performances between the standard and modified versions of *air2water* in three selected years. While the difference for the time series of δ is evident (Figure 7b),

Table 1
Comparison Between the Standard Formulation of air2water With δ Expressed by Equation 5 and the Version Modified Using Equation 9, for the Original "Deep" Case Inspired by Lake Zurich and for the Alternative Cases Characterized by Two Different (Intermediate and Shallow) Depths

Case	Deep (original)		Intermediate		Shallow	
Formulation for δ	Equation 5	Equation 9	Equation 5	Equation 9	Equation 5	Equation 9
Number of parameters	6	9	6	9	6	9
RMSE [°C]	0.961	0.892	0.819	0.799	0.745	0.716
AIC[a]	−951	−2,727	−4,808	−5,390	−7,081	−8,029
a [°C]	8.93	3.51	11.2	7.39	66.0	51.0
a_{as} [–]	–	0.0685	–	0.118	–	0.798
a_T [°C]	–	6.85	–	7.08	–	0.371
a_δ [–]	–	0.393	–	0.543	–	0.761

[a]The Akaike Information Criterion (AIC) was computed as $AIC = 2N\ ln\ RMSE + 2p$, where N (= 12,053) is the number of data and p is the number of model's parameters. Lower values indicate better performance.

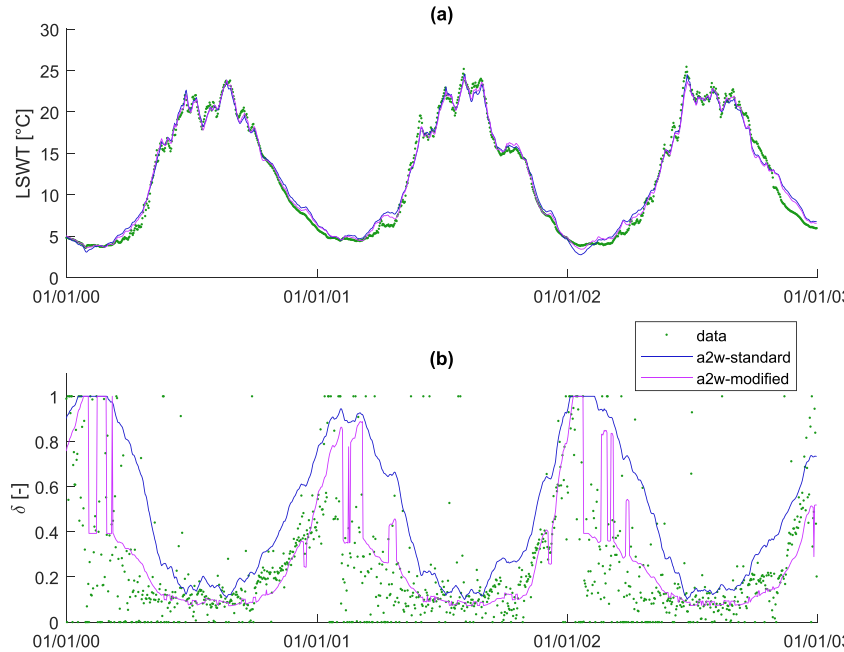

Figure 7. Reconstruction of simulated LSWT for 3 years (2000–2002): (a) using *air2water* with the standard formulation (Equation 5) and the dual dependence (Equation 9) for δ; subplot (b) shows the effect on δ. Note that in this period, the performance of *air2water* is remarkable and the modified version allows for a significant improvement: RMSE is 0.821 and 0.708°C for the standard and the modified version, respectively. LSWT, lake surface water temperature.

with the smaller values of the modified version during the warming period (reducing δ), the effect on the prediction of LSWT is not immediately visible, although it is substantial in numbers (RMSE improving from 0.821 to 0.708°C in the 3 years). The definition of the warming and cooling phases is based on a limited window of previous days and produces some fluctuations of δ in Figure 7b, but allows for reproducing the values computed from the heat budget more accurately.

3.4. How Depth Affects Stratification and δ

The use of a model to generate the time series of LSWT allowed us to explore the influence of different factors on the thermal response of a lake. Here we focus on the effect of lake depth, which in turn controls the development of stratification in the warm season. As anticipated, if the lake is deep enough, during stratified periods, a surface layer is thermally isolated from the deeper region and, hence, reduces the heat capacity that controls LSWT. Conversely, in shallow lakes, the thickness of the surface layer that would develop in response to the same external forcing is larger than the maximum depth. These lakes are often well-mixed (polymictic) and only occasionally show a locally stratified temperature profile. Thus, the dependence of δ on LSWT can be different from what we have seen so far. Moreover, in clear shallow lakes, a fraction of the penetrative short-wave radiation can reach the lake bottom, a condition that is not considered in most of the available models. To understand how the thermal response can change, we examine two cases with different depths, but with the same surface area and a vertical coordinate that is stretched from the surface to the maximum depth (see Table S1 in Supporting Information S1; see also Figures S11–S19 and S21–S30 in Supporting Information S1).

First, we examine the intermediate case with a maximum depth of 50 m (Figure 8a), which is similar to the deep case (Figure 6). In both cases, two different limbs of the hysteresis can be distinguished, one for the warming phase (with lower values of δ) and one for the cooling phase (higher δ). The peak of δ is reached in the range of temperature that approximately corresponds to the deep water temperature (compare Figure 6 with Figure S3 and Figure 8a with Figure S9 in Supporting Information S1), that is, around 5°C in the former case and variable between approximately 5 and 10°C in the latter case. However, for this intermediate depth, a difference is clearly visible between the peaks of δ at the start of the warming phase (when LSWT is initially colder than T_{md}), and the maximum δ that occurs when the whole lake volume becomes homothermal at the end of the cooling phase (when

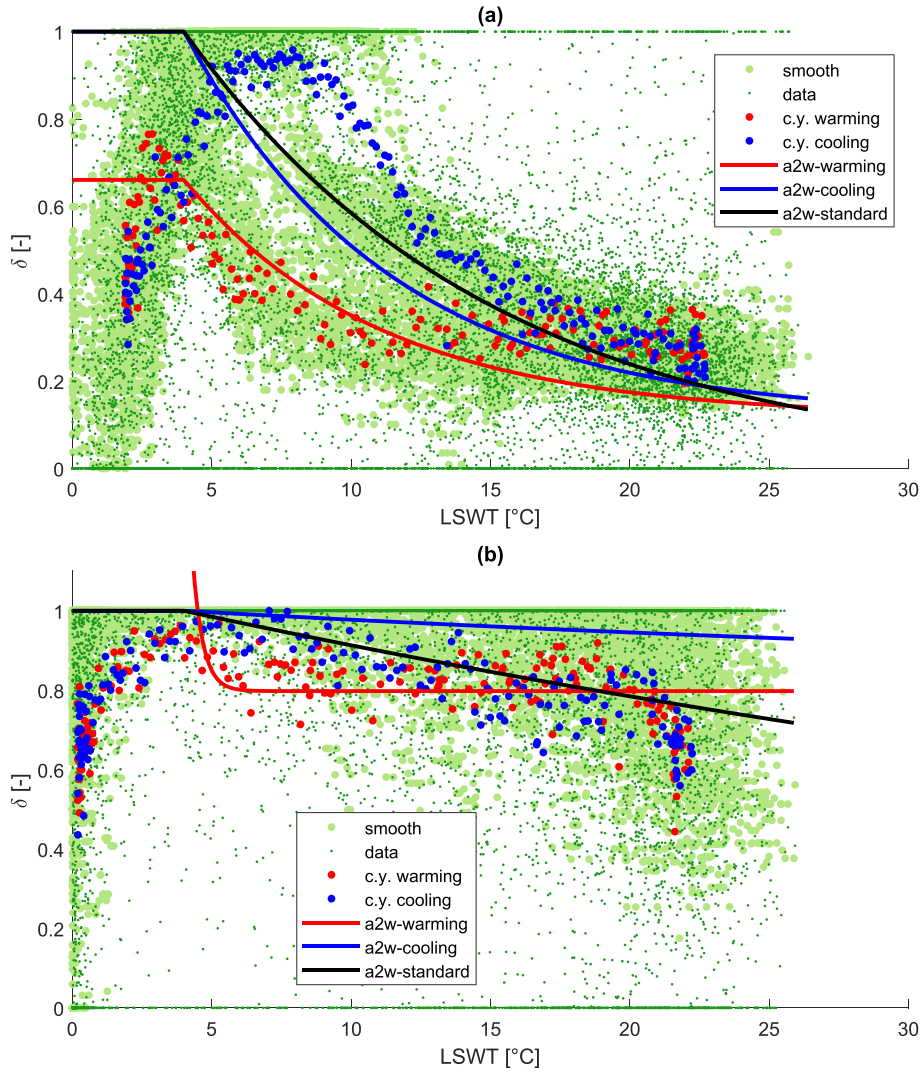

Figure 8. The same plot as in Figure 6, but for the case of (a) intermediate depth (maximum depth 50 m) and (b) shallow depth (maximum depth 10 m). In the latter case, the constant value of δ for LSWT < 4°C is larger than 1 in the warming phase (1.559 from the calibrated values in Table 1). LSWT, lake surface water temperature.

deep water temperature is warmer than T_{md} because of progressive heating of the hypolimnion during summer). This behavior is not captured by the *air2water* parameterization, which imposes the same value of $T_h = 4$°C for dimictic lakes.

As for the deep case, in Figure 8a, an asymptotic tendency can be noted for δ as LSWT becomes warmer. By rescaling the asymptotic values $\delta \sim 0.1$ (deep case) and $\delta \sim 0.25$ (intermediate depth) using the hypsometric curve, it is possible to obtain a reference value of the depth of the thermally reactive layer in strongly stratified conditions. Interestingly, the thickness of this surface layer is approximately 5 m in both cases, an indication that this depth is likely determined by the external forcing (penetration of shortwave radiation and wind-induced mixing as main factors), and not by the lake depth.

How does the shallow case behave, then? For the 10-m-deep case, the average depth (3.69 m) is comparable with the estimate of the minimum depth of the surface layer that we have just obtained by looking at the other cases, suggesting that it is difficult to isolate the surface layer from the deep water. Indeed, the shallow case is well-mixed throughout the whole year (Figure S20 in Supporting Information S1), so that the variability of δ with LSWT for the climatic year (blue and red dots) is lower than that in the other cases (Figure 8b). The values of δ computed with Equation 6 significantly deviate from unity only for very cold (close to freezing) or very warm

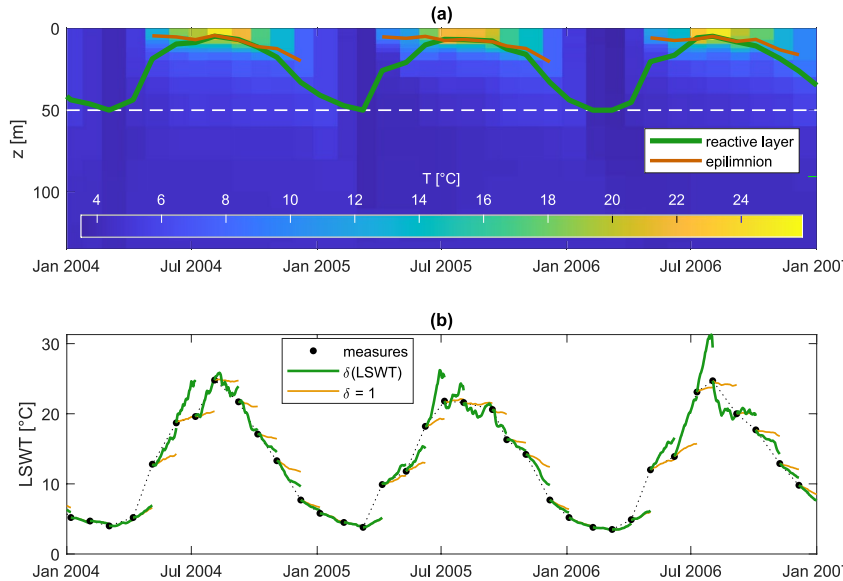

Figure 9. Temporal evolution of the water temperature from monthly observations in the real Lake Zurich in 3 years (2004–2006). (a) Time-depth plot of observed temperature, with the indication of the depth of the epilimnion (computed according to the method described in Section 2.3) and of the thermally reactive layer (estimated by computing δ with the measured LSWT according to Equation 5); the horizontal dashed white line indicates the average depth. (b) Variability of monthly measured LSWT (black dots) and its reconstruction based on the heat budget (Equation 3) with $V_r = \delta V_{tot}$ and using δ variable with LSWT (green curve) and a constant value $\delta = 1$. LSWT, lake surface water temperature.

LSWT, and anyway they are always larger than 0.5. Therefore, the parameterization of δ in shallow lakes does not require complex formulations. The use of Equation 9 leads to unexpected results, like the two-stage curve for the warming phase with calibrated values of $\delta > 1$ for LSWT <4°C. Finally, we note that the minor relevance of accounting for the seasonally varying stratification in the shallow and intermediate cases is confirmed by the lower improvement obtained using Equation 9 instead of Equation 5 (see Table 1).

3.5. A Comparison With Actual Observations

So far, the analysis was based exclusively on the results of numerical simulations. In this section, we extend the discussion to a comparison with observations from a real lake. To this end, we rely on the water temperature profiles measured on a monthly basis in Lake Zurich, that is, the same lake that was assumed as a reference for the numerical model.

Figure 9a shows the formation and disruption of the stratification in Lake Zurich as obtained from the measured water temperature profiles in 3 selected years (2004–2006). The plot also reports the epilimnion depth computed with the same method as before (strongest temperature gradient), but using the measured profiles, and the variability of the thermally reactive layer δD_{av}, with $D_{av} \cong 50.1$ m being the mean depth of the lake. In this computation, δ was estimated by means of Equation 5 with the observed LSWT and the parameter a calibrated for the synthetic case (Table 1). It is possible to recognize that the thermally reactive layer approximately coincides with the epilimnion during the period of maximum stratification in summer, while it tends to its maximum value (D_{av} corresponding to $\delta = 1$) when the water column is well-mixed. The epilimnion thickness continuously grows from spring to fall. Conversely, the reactive layer is thicker in spring (the estimate might be slightly modified by using the dual formulation as in Equation 9, but the tendency is similar). In fact, the stratification is weak and mostly superficial at the beginning of the warming phase: the inhibition of turbulent fluxes is not as efficient as in fall when the thickening of the epilimnion is mostly due to convective destratification, which maintains a strong thermocline that only shifts downwards.

Figure 9b is focused on LSWT. Observed temperatures follow the classical sinusoidal-like behavior, but the monthly resolution is not sufficient to appreciate the actual variability. We tried to reconstruct the daily variability, for approximately 1 month, starting from the days when measurements were available. In this exercise, we

adopted the net heat flux computed by Simstrat (which may be significantly different from the actual one because it depends on the simulated LSWT) and we computed LSWT day by day based on the heat budget in Equation 3, where we replaced V_r by δV_{tot} and considered both δ variable with LSWT and a constant value $\delta = 1$. The reconstructed LSWT follows the observations reasonably well, apart from some large discrepancies that might be due to both the deficiencies of this simplified heat budget approach and the inaccurate quantification of the net heat flux, which especially does not account for the feedback produced by a wrong LSWT. Nevertheless, it appears that considering the variability of the thermally reactive layer (through δ) is absolutely necessary, as it is emphasized by the comparison with the same type of reconstruction obtained by imposing $\delta = 1$.

4. Discussion and Conclusions

The concept of a thermally reactive surface layer in lakes is based on the physical intuition that a strong density gradient inhibits turbulence and hence the vertical fluxes of mass, momentum, and energy (heat). In fact, the capacity to store the heat transferred through the lake surface into this layer is the factor that controls the rate of warming/cooling of LSWT. Despite the relevance of this mechanism, we are not aware of any attempt to quantify and relate it to the most relevant factors. In this sense, the introduction of the dimensionless parameter δ was the most important novelty in the *air2water* model originally proposed by Piccolroaz et al. (2013). By introducing this element belonging to the physics of the system, even if in a very simple way, *air2water* acquires a dramatic advantage with respect to standard stochastic models, as confirmed by several works that showed how *air2water* typically outperforms other models of similar complexity, including recent machine learning algorithms (Heddam et al., 2020; Yousefi & Toffolon, 2022; Zhu et al., 2020). Therefore, the functional dependence of δ on LSWT deserved a deeper analysis.

In this study, exploiting the availability of all the relevant data resulting from the use of a physically based model (Simstrat) instead of observations, we have shown how the thermally reactive volume changes with LSWT, and hence with the season. Typically, it shrinks in stratified summer conditions: the surface layer is thermally insulated by the thermocline underneath; the heat capacity of the water reacting to the net heat flux reduces, and eventually, the changes of LSWT are amplified (Calamita et al., 2021; Piccolroaz et al., 2015; Woolway & Merchant, 2017; Zhong et al., 2016). This simplified description explains why LSWT is characterized by much larger fluctuations in summer than in winter.

The analysis has shown that δ decreases with LSWT from the conditions of lake overturn (LSWT close to the deep-water temperature) until reaching the lowest values for the warmest LSWT, for which δ can decrease by an order of magnitude. The dependence can be approximated by an exponential function, as done in *air2water*, but a more accurate description requires a separate treatment of the warming period (spring-summer, when LSWT grows) and of the cooling period (fall-winter, when LSWT drops). Our results suggest a tendency toward an asymptotic value of δ for the warmest LSWT, and we speculate that this can be determined by water transparency (affecting the penetration of shortwave radiation) and wind-induced mixing (e.g., Imberger, 1985).

The improvement of the performances obtained by using the parameterization in Equation 9 in a model like *air2water* is significant, but it might require additional care in the calibration of the model due to the additional parameters introduced in the formulation (Zhu et al., 2021). In this respect, our results show that the fixed parameterization of the deep-water temperature adopted in *air2water* (fixed at T_{md} if LSWT falls below this value during the cold season) is not optimal for lakes with shallow or intermediate depths. In fact, in these cases, the deep-water temperature can change during summer and a coupled model for the lake's bottom layer would be necessary to follow the dynamics. Anyway, in the case of very shallow lakes, a fixed value of δ could be safely adopted (see also Figure S30 in comparison with Figures S8 and S19 in Supporting Information S1). Finally, we also note that we focused only on the effect of direct stratification (LSWT $> T_{md}$) and further work is required to provide a more reliable model for δ in the period of inverse stratification (LSWT $< T_{md}$) with respect to the existing 8-parameter version of *air2water* (not tested in this study). This issue is more relevant if lakes in cold climates are considered.

The analysis of the variability of δ with LSWT shed new light on the process of stratification in lakes. By confirming a conceptual model that predicts more intense LSWT response to surface heat fluxes in warmer waters, in line with recent works suggesting increasing maximum LSWT under past and future decades (Dokulil et al., 2021; Piccolroaz et al., 2021), our results suggest that positive feedback can establish in a warming climate.

Warmer LSWT that persists for longer periods will create the condition for a fast response of LSWT to the increasingly warmer air temperature, following and further contributing to a reduced thermal inertia that can otherwise limit the LSWT peaks. Indeed, understanding the processes leading to the LSWT warming rate is of paramount importance for the interpretation of the effects of climate change on water bodies and on the ecosystems developing therein.

Data Availability Statement

The code (Simstrat v2.4.1) and the data used for the simulation of the reference case based on Lake Zurich (CH) were downloaded from https://simstrat.eawag.ch/. The *air2water* model can be downloaded from https://doi.org/10.5281/zenodo.254590 (Piccolroaz & Toffolon, 2017).

Acknowledgments
Data from Lake Zurich were provided by the City of Zurich Water Supply and by the Amt für Abfall, Wasser, Energie und Luft of the Canton of Zurich. Open Access Funding provided by Universita degli Studi di Trento within the CRUI-CARE Agreement.

References

Anderson, E. J., Stow, C. A., Gronewold, A. D., Mason, L. A., McCormick, M. J., Qian, S. S., et al. (2021). Seasonal overturn and stratification changes drive deep-water warming in one of Earth's largest lakes. *Nature Communications*, *12*(1), 1688. https://doi.org/10.1038/s41467-021-21971-1

Butcher, J. B., Nover, D., Johnson, T. E., & Clark, C. M. (2015). Sensitivity of lake thermal and mixing dynamics to climate change. *Climatic Change*, *129*(1), 295–305. https://doi.org/10.1007/s10584-015-1326-1

Calamita, E., Piccolroaz, S., Majone, B., & Toffolon, M. (2021). On the role of local depth and latitude on surface warming heterogeneity in the Laurentian Great Lakes. *Inland Waters*, *11*(2), 208–222. https://doi.org/10.1080/20442041.2021.1873698

Czernecki, B., & Ptak, M. (2018). The impact of global warming on lake surface water temperature in Poland – The application of empirical-statistical downscaling, 1971-2100. *Journal of Limnology*, *77*, 330–348. https://doi.org/10.4081/jlimnol.2018.1707

Delpla, I., Jung, A.-V., Baures, E., Clement, M., & Thomas, O. (2009). Impacts of climate change on surface water quality in relation to drinking water production. *Environment International*, *35*(8), 1225–1233. https://doi.org/10.1016/j.envint.2009.07.001

Dokulil, M. T., de Eyto, E., Maberly, S. C., May, M., Weyhenmeyer, G. A., & Woolway, R. I. (2021). Increasing maximum lake surface temperature under climate change. *Climatic Change*, *165*(56). https://doi.org/10.1007/s10584-021-03085-1

Fang, X., & Stefan, H. G. (1996). Dynamics of heat exchange between sediment and water in a lake. *Water Resources Research*, *32*(6), 1719–1727. https://doi.org/10.1029/96wr00274

Ficker, H., Luger, M., & Gassner, H. (2017). From dimictic to monomictic: Empirical evidence of thermal regime transitions in three deep alpine lakes in Austria induced by climate change. *Freshwater Biology*, *62*(8), 1335–1345. https://doi.org/10.1111/fwb.12946

Flaim, G., Andreis, D., Piccolroaz, S., & Obertegger, U. (2020). Ice cover and extreme events determine dissolved oxygen in a placid mountain lake. *Water Resources Research*, *56*, e2020WR027321. https://doi.org/10.1029/2020wr027321

Gaudard, A., Råman Vinnå, L., Bärenbold, F., Schmid, M., & Bouffard, D. (2019). Toward an open access to high-frequency lake modeling and statistics data for scientists and practitioners–the case of Swiss lakes using Simstrat v2. 1. *Geoscientific Model Development*, *12*(9), 3955–3974. https://doi.org/10.5194/gmd-12-3955-2019

Golub, M., Thiery, W., Marcé, R., Pierson, D., Vanderkelen, I., Mercado, D., et al. (2022). A framework for ensemble modelling of climate change impacts on lakes worldwide: The ISIMIP Lake Sector. *Geoscientific Model Development*, *15*, 4597–4623. https://doi.org/10.5194/gmd-15-4597-2022

Goudsmit, G. H., Burchard, H., Peeters, F., & Wüest, A. (2002). Application of k-ϵ turbulence models to enclosed basins: The role of internal seiches. *Journal of Geophysical Research: Oceans*, *107*(C12), 23-1–23-13. https://doi.org/10.1029/2001jc000954

Heddam, S., Ptak, M., & Zhu, S. (2020). Modelling of daily lake surface water temperature from air temperature: Extremely randomized trees (ERT) versus Air2Water, MARS, M5Tree, RF and MLPNN. *Journal of Hydrology*, *588*, 125130. https://doi.org/10.1016/j.jhydrol.2020.125130

Hondzo, M., & Stefan, H. G. (1993). Regional water temperature characteristics of lakes subjected to climate change. *Climatic Change*, *24*(3), 187–211. https://doi.org/10.1007/bf01091829

Imberger, J. (1985). The diurnal mixed layer. *Limnology & Oceanography*, *30*(4), 737–770. https://doi.org/10.4319/lo.1985.30.4.0737

IPCC. (2021). Summary for policymakers. In V., MassonDelmotte, P., Zhai, A., Pirani, S. L., Connors, C., Péan, S., Berger, et al. (Eds.), *Climate change 2021: The physical science basis. Contribution of working group I to the sixth assessment report of the intergovernmental panel on climate change [MassonDelmotte*. Cambridge University Press.

Javaheri, A., Babbar-Sebens, M., & Miller, R. N. (2016). From skin to bulk: An adjustment technique for assimilation of satellite-derived temperature observations in numerical models of small inland water bodies. *Advances in Water Resources*, *92*, 284–298. https://doi.org/10.1016/j.advwatres.2016.03.012

Lofgren, B. M., & Zhu, Y. (2000). Surface energy fluxes on the Great Lakes based on satellite-observed surface temperatures 1992 to 1995. *Journal of Great Lakes Research*, *26*(3), 305–314. https://doi.org/10.1016/s0380-1330(00)70694-0

Magnuson, J. J., Robertson, D. M., Benson, B. J., Wynne, R. H., Livingstone, D. M., Arai, T., et al., (2000). Historical trends in lake and river ice cover in the Northern Hemisphere. *Science*, *289*(5485), 1743–1746. https://doi.org/10.1126/science.289.5485.1743

McCombie, A. M. (1959). Some relations between air temperatures and the surface water temperatures of lakes. *Limnology & Oceanography*, *4*(3), 252–258. https://doi.org/10.4319/lo.1959.4.3.0252

Nehorai, R., Lensky, L., Brenner, S., & Lensky, I. (2013). The dynamics of the skin temperature of the Dead Sea. *Advances in Meteorology*, 296714. https://doi.org/10.1155/2013/296714

Paerl, H. W., & Huisman, J. (2008). Climate: Blooms like it hot. *Science*, *320*(5872), 57–58. https://doi.org/10.1126/science.1155398

Piccolroaz, S. (2016). Prediction of lake surface temperature using the air2water model: Guidelines, challenges, and future perspectives. *Advances in Oceanography and Limnology*, *7*(1). https://doi.org/10.4081/aiol.2016.5791

Piccolroaz, S., Healey, N. C., Lenters, J. D., Schladow, S. G., Hook, S. J., Sahoo, G. B., & Toffolon, M. (2018). On the predictability of lake surface temperature using air temperature in a changing climate: A case study for Lake Tahoe (U.S.A.). *Limnology & Oceanography*, *63*, 243–261. https://doi.org/10.1002/lno.10626

Piccolroaz, S., & Toffolon, M. (2017). spiccolroaz/air2water: air2water 2.0 (v2.0.0). Zenodo. https://doi.org/10.5281/zenodo.254590

Piccolroaz, S., Toffolon, M., & Majone, B. (2013). A simple lumped model to convert air temperature into surface water temperature in lakes. *Hydrology and Earth System Sciences*, *17*(8), 3323–3338. https://doi.org/10.5194/hess-17-3323-2013

Piccolroaz, S., Toffolon, M., & Majone, B. (2015). The role of stratification on lakes' thermal response: The case of Lake Superior. *Water Resources Research*, *51*(10), 7878–7894. https://doi.org/10.1002/2014wr016555

Piccolroaz, S., Woolway, R. I., & Merchant, C. J. (2020). Global reconstruction of 20th century lake surface water temperature reveals different warming trends depending on the climatic zone. *Climatic Change*, *160*, 427–442. https://doi.org/10.1007/s10584-020-02663-z

Piccolroaz, S., Zhu, S., Ptak, M., Sojka, M., & Du, X. (2021). Warming of lowland Polish lakes under future climate change scenarios and consequences for ice cover and mixing dynamics. *Journal of Hydrology: Regional Studies*, *34*, 100780. https://doi.org/10.1016/j.ejrh.2021.100780

Prats, J., & Danis, P. A. (2019). An epilimnion and hypolimnion temperature model based on air temperature and lake characteristics. *Knowledge and Management of Aquatic Ecosystems*, *420*, 809–813. https://doi.org/10.1051/kmae/2019001

Prats, J., Reynaud, N., Rebière, D., Peroux, T., Tormos, T., & Danis, P. A. (2018). LakeSST: Lake skin surface temperature in French inland water bodies for 1999-2016 from Landsat archives. *Earth System Science Data*, *10*, 727–743. https://doi.org/10.5194/essd-10-727-2018

Sahoo, G. B., Forrest, A. L., Schladow, S. G., Reuter, J. E., Coats, R., & Dettinger, M. (2016). Climate change impacts on lake thermal dynamics and ecosystem vulnerabilities. *Limnology & Oceanography*, *61*(2), 496–507. https://doi.org/10.1002/lno.10228

Sakamoto, Y., Ishiguro, M., & Kitagawa, G. (1986). *Akaike information criterion statistics*. D. Reidel Publishing Co. https://doi.org/10.1080/01621459.1988.10478680

Schmid, M., Hunziker, S., & Wüest, A. (2014). Lake surface temperatures in a changing climate: A global sensitivity analysis. *Climatic Change*, *124*(1), 301–315. https://doi.org/10.1007/s10584-014-1087-2

Schmid, M., & Köster, O. (2016). Excess warming of a Central European lake driven by solar brightening. *Water Resources Research*, *52*, 8103–8116. https://doi.org/10.1002/2016wr018651

Toffolon, M., Piccolroaz, S., & Calamita, E. (2020). On the use of averaged indicators to assess lakes' thermal response to changes in climatic conditions. *Environmental Research Letters*, *15*(3), 034060. https://doi.org/10.1088/1748-9326/ab763e

Toffolon, M., Piccolroaz, S., Majone, B., Soja, A. M., Peeters, F., Schmid, M., & Wüest, A. (2014). Prediction of surface temperature in lakes with different morphology using air temperature. *Limnology & Oceanography*, *59*(6), 2185–2202. https://doi.org/10.4319/lo.2014.59.6.2185

Wilson, H. L., Ayala, A. I., Jones, I. D., Rolston, A., Pierson, D., de Eyto, E., et al. (2020). Variability in epilimnion depth estimations in lakes. *Hydrology and Earth System Sciences*, *24*(11), 5559–5577. https://doi.org/10.5194/hess-24-5559-2020

Wilson, R. C., Hook, S. J., Schneider, P., & Schladow, S. G. (2013). Skin and bulk temperature difference at Lake Tahoe: A case study on lake skin effect. *Journal of Geophysical Research – Atmosphere*, *118*, 10332–10346. https://doi.org/10.1002/jgrd.50786

Wood, T. M., Wherry, S. A., Piccolroaz, S., & Girdner, S. F. (2016). Simulation of deep ventilation in Crater Lake, Oregon, 1951–2099. U.S. Geological Survey Scientific Investigations Report 2016-5046, 43. https://doi.org/10.3133/sir20165046

Woolway, R. I., & Merchant, C. J. (2017). Amplified surface temperature response of cold, deep lakes to inter-annual air temperature variability. *Scientific Reports*, *7*(1), 1–8. https://doi.org/10.1038/s41598-017-04058-0

Woolway, R. I., Sharma, S., Weyhenmeyer, G. A., Debolskiy, A., Golub, M., Mercado-Bettín, D., et al. (2021). Phenological shifts in lake stratification under climate change. *Nature Communications*, *12*(1), 2318. https://doi.org/10.1038/s41467-021-22657-4

Yousefi, A., & Toffolon, M. (2022). Critical factors for the use of machine learning to predict lake surface water temperature. *Journal of Hydrology*, *606*, 127418. https://doi.org/10.1016/j.jhydrol.2021.127418

Zhong, Y., Notaro, M., Vavrus, S. J., & Foster, M. J. (2016). Recent accelerated warming of the Laurentian Great Lakes: Physical drivers. *Limnology & Oceanography*, *61*(5), 1762–1786. https://doi.org/10.1002/lno.10331

Zhu, S., Piotrowski, A. P., Ptak, M., Napiorkowski, J. J., Daid, J., & Jia, Q. (2021). How does the calibration method impact the performance of the air2water model for the forecasting of lake surface water temperatures? *Journal of Hydrology*, *597*, 126219. https://doi.org/10.1016/j.jhydrol.2021.126219

Zhu, S., Ptak, M., Yaseen, Z. M., Dai, J., & Sivakumar, B. (2020). Forecasting surface water temperature in lakes: A comparison of approaches. *Journal of Hydrology*, *585*, 124809. https://doi.org/10.1016/j.jhydrol.2020.124809